The Conformational Structure of Bovine Serum Albumin Layers Adsorbed at the Silica−Water Interface

T. J. Su and J.R. Lu*

Department of Chemistry, University of Surrey, Guildford GU2 5XH, U.K.

R. K. Thomas

Physical and Theoretical Chemistry Laboratory, South Parks Road, Oxford OX1 3QZ, U.K.

Z. F. Cui

Department of Engineering Science, Parks Road, Oxford OX1 3PJ, U.K.

J. Penfold

ISIS, CCLRC, Chilton, Didcot OX11 0QX, U.K.

Received: February 22, 1998; In Final Form: May 13, 1998

The adsorption of bovine serum albumin (BSA) at the hydrophilic silica−water interface has been studied using specular neutron reflection. The measurements were made over the concentration range from 0.005 to 0.5 $g\ dm^{-3}$. The surface excess was found to vary from 1.8 to 2.4 $mg\ m^{-2}$. The layers could be modeled using a single uniform layer model, suggesting that over the concentration range studied there is insignificant denaturation, which would lead to a more fragmented peptide distribution and hence layers of different density. Comparison of the layer thickness with the dimensions of the ellipsoidal structure of the globular solution structure indicates that the molecules adsorb sideways-on. Nevertheless, the layer thickness is always less than 40 Å, suggesting that adsorption onto the hydrophilic surface results in some structural deformation. The increase of layer thickness with bulk concentration suggests that the extent of the distortion is reduced as the lateral repulsion between protein molecules increases. The effect of pH on the adsorbed BSA layer was examined by varying the pH at a fixed BSA concentration of 0.15 $g\ dm^{-3}$. The cycle was started at a pH of 5.1, followed by pH 7, 5.1, 3, and then back to 5.1. The neutron reflectivity profiles showed no hysteresis in either adsorbed amount or structure. The reversibility of the adsorption of BSA with respect to pH is consistent with no denaturation occurring on the surface. The adsorbed amount was a maximum at pH 5.1, which is close to the isoelectric point at pH 4.8.

Introduction

On a hydrophilic solid substrate, the electrostatic attraction between a charged surface and an oppositely charged protein molecule is often the driving force for adsorption from solution on to the solid surface. The amount finally adsorbed may then be determined by a balance between this electrostatic attraction and the electrostatic repulsion within the adsorbed layer.[1−3] On a hydrophobic surface, the attraction is between the hydrophobic surface and hydrophobic fragments within the protein and this may be sufficiently strong to dominate electrostatic interactions to the extent that adsorption may occur even when the charge on the solid surface and the protein are the same. A further driving force for protein adsorption has been attributed to entropic changes associated with dehydration of the protein and solid surface and/or structural rearrangement within the protein. These changes may be sufficient to cause adsorption on a hydrophilic surface in the absence of hydrophobic forces even when there is charge repulsion between the solid surface and protein.[1,4]

Strong surface interactions may damage the native state of a protein molecule and lead to the loss of its coherent structure. The extent of structural deformation on adsorption depends on the nature of the surface and the relative stability of the protein structure. Structural changes in proteins following adsorption have been detected in many cases (for example, refs 5−10). The main observation which suggests perturbation to the secondary and tertiary structure is a decrease in α-helix content. Loss of helical structure is likely to increase flexibility within the polypeptide chain with a consequent increase in the conformational entropy of the protein molecule. Using differential microcalorimetry Haynes *et al.*[11] have examined the structural pertubation and thermodynamic stability of hen egg-white lysozyme and bovine milk α-lactabumin, both of which are globular and of similar size, and have shown that dehydration of the solid surface and protein molecules provides a substantial entropic driving force for adsorption. Significant denaturation was observed for both proteins adsorbed on a hydrophobic polystyrene surface. In contrast, lysozyme only loses a small fraction of its secondary structure when adsorbed onto the hydrophilic α-Fe_2O_3 surface, although α-lactabumin was found to denature almost completely. These differences are consistent

* To whom all correspondence should be addressed: Department of Chemistry, University of Surrey, Guildford GU2 5XH, U.K.

S1089-5647(98)01239-5 CCC: $15.00
Published on Web 09/19/1998

with the high structural stability of the native state of lysozyme. Structural changes on adsorption have also been measured by circular dichroism. For example, Kondo et al.[12] have compared structural changes of several globular proteins adsorbed on silicon powder from buffered aqueous solution. Little structural change was observed for robust globular proteins such as cytochrome c and ribonuclease A, but loss of helical content was detected for more flexible proteins such as bovine serum albumin (BSA) and hemoglobin.

Structural information (*e.g.*, layer thickness and protein density distributions) may be more accessible at flat interfaces. For example, Fitzpatrick *et al.*[13] have used a surface force apparatus to measure the structural conformation of a BSA layer adsorbed at the mica−water interface and concluded from the thickness of 120 Å for the adsorbed layer that BSA molecule adsorbs with its long axis vertical at this interface. Using the same technique, Gallinet *et al.*[14] studied BSA adsorption on mica under almost identical conditions and found three steps in the surface force−distance curve, each corresponding to the detachment of a BSA layer. The thickness of the steps was about 44 Å, indicating that the adsorbed layer consists of three BSA layers with the molecules adsorbed sideways-on. The conflict between these measurements must mean that at least one of the conclusions must be wrong.

Specular neutron reflection has recently been applied to the study of proteins adsorbed at the solid−water interface. The depth resolution of neutron reflection is higher than most techniques presently being used, which stems from two factors. First, the neutron wavelength is much shorter than that of light at 1−10 Å, which is comparable with the dimensions of the protein layers to be probed. Second, isotopic substitution can be used to vary the contrast between water, protein, and solid substrate so that the adsorbed protein layer is highlighted. Furthermore, variation between H_2O and D_2O also allows a reliable determination of the extent to which water penetrates the protein layer. This information combined with the known dimensions of globular proteins often allows conclusions to be drawn about the physical state of an adsorbed protein layer. Thus, neutron reflection has recently been used to examine adsorption of hen egg-white lysozyme on a bare silica surface and on the hydrophobic surface obtained by chemical grafting of a self assembled monolayer of octadecyltrichlorosilane (OTS).[2,15] While lysozyme on the hydrophilic oxide surface retains its native structure the adsorbed protein layer on hydrophobic OTS was seriously denatured. Neutron reflectivity data also showed that lysozyme was reversibly adsorbed on the hydrophilic surface with respect to solution pH variation,[2] but adsorption onto the hydrophobic OTS was completely irreversible.[15]

We now extend these neutron reflection experiments to BSA on a flat surface. The globular structure of BSA in aqueous solution has been extensively studied by various techniques including small angle x-ray scattering (SAXS),[16−17] quasielastic light scattering (QELS),[18] and small angle neutron scattering (SANS).[19] An extensive review on BSA structure and solution properties has been presented by Peters.[20] BSA has three main domains, which can be further divided into six subdomains. The molecule is approximately a prolate ellipsoid with major and minor axes respectively equal to 140 and 40 Å. The net charge in each main domain is different and pH dependent so that pH variation can affect the shape and structure of the molecule. We examine adsorption of BSA at the hydrophilic silica oxide−water interface at a resolution where any structural deformation upon adsorption should be detectable. We have also investigated the reversibility of adsorption with respect to solution pH, which gives indirect information about the extent of denaturation.

Experimental Section

The neutron reflection measurements were made on the white beam reflectometer CRISP at the Rutherford-Appleton Laboratory, ISIS, Didcot, U.K.,[21] using neutron wavelengths from 1−6 Å. The sample cell was almost identical to that depicted by Fragneto *et al.* in ref 22 with the aqueous solution contained in a teflon trough clamped against a silicon block of dimensions $12.5 \times 5 \times 2.5$ cm^3. The collimated beam enters the end of the silicon block at a fixed angle, is reflected at a glancing angle from the solid−water interface, and exits from the opposite end of the silicon block. Each reflectivity profile was measured at three different glancing angles, 0.35°, 0.8°, and 1.8°, and the results combined. The beam intensity was calibrated with respect to the intensity below the critical angle for total reflection at the silicon−D_2O interface. A flat background determined by extrapolation to high values of momentum transfer κ ($\kappa = (4\pi \sin\theta)/\lambda$, where λ is the wavelength and θ is the glancing angle of incidence) was subtracted. For all the measurements, the reflectivity profiles were essentially flat at $\kappa > 0.2$ Å^{-1}, although the limiting signal at this point was dependent on the H_2O/D_2O ratio. The typical background for D_2O runs was found to be 2×10^{-6} and that for H_2O to be 3.5×10^{-6} (measured in terms of the reflectivity).

Fatty acid free BSA sample was purchased from Sigma and used as supplied (catalogue no. A0281, lot no. 10H9304). The molecular weight of BSA is 66700 ± 400. D_2O (99.9% D) was obtained from Fluorochem and its surface tension was typically over 71 *mN m*$^{-1}$ at 298 *K*, indicating the absence of any surface active impurity. H_2O was processed through an Elgastat ultrapure water system (UHQ) and its surface tension at 298 *K* was constant at 71.5 *mN m*$^{-1}$. The solution pH was controlled by using phosphate buffer and the pH varied by changing the concentration ratio of Na_2HPO_4, NaH_2PO_4 and H_3PO_4, keeping the total ionic strength fixed at 0.02 *M*. There were small differences in pH between H_2O and D_2O but this was controlled to within 0.2 pH units. The glassware and Teflon troughs for the reflection measurements were cleaned using alkaline detergent (Decon 90) followed by repeated washing in UHQ water. All the experiments were performed at 298 *K*.

The large (111) face of each silicon block was polished using an Engis polishing machine. The blocks were lapped on a copper plate with 3 micron diamond polishing fluid and on a pad with 1 micron diamond followed by 0.1 micron alumina suspension. The freshly polished surfaces were immersed in neutral Decon solution (5%) and ultrasonically cleaned for 30 minutes and this was followed by a further 30 min of ultrasonic cleaning in water. The blocks were then copiously rinsed and soaked in acid peroxide solution (600 mL 98% H_2SO_4 in 100 mL 25% H_2O_2) for 6 min at 120 °C.[23] The blocks were then thoroughly rinsed with UHQ water to remove acid, and exposed to UV/ozone for 30 min to remove any traces of organic impurities.[24] They were then left to soak in UHQ water for at least 24 h. This procedure was found to produce surfaces with reproducible thickness and roughness of the oxide layer, which were completely wetted by water. The reproducibility in surface hydrophilicity between different blocks was tested by measuring reflectivity profiles from lysozyme adsorbed from a solution of 0.03 *g dm*$^{-3}$ lysozyme in D_2O, which always gave a good fit to a thickness of 30 ± 3 Å and a coverage of 1.9 ± 0.2 *mg m*$^{-2}$.

Neutron Reflection. The reflectivity of neutrons $R(\kappa)$ is approximately determined by the variation of scattering length density $\rho(z)$ along the surface normal direction:[25,26]

$$R(\kappa) = \frac{16\pi^2}{\kappa^2}|\hat{\rho}(\kappa)|^2 \quad (1)$$

where $\hat{\rho}(\kappa)$ is the one-dimensional Fourier transform of $\rho(z)$

$$\hat{\rho}(\kappa) = \int_{-\infty}^{\infty} \exp(-i\kappa z)\rho(z)\, dz \quad (2)$$

The scattering length density depends on the chemical composition through the equation

$$\rho = \Sigma n_i b_i \quad (3)$$

where n_i is the number density of element i and b_i its scattering amplitude (scattering length). Because values of b_i vary between isotopes, isotopic substitution can be used to change the reflectivity from a given chemical structure, and this can be a great help in revealing the structural details of an interface. This is particularly the case for systems containing hydrogen atoms. For example, the scattering lengths of D and H are of opposite sign and hence the scattering length density of water can be varied over a wide range, which can be used to highlight an adsorbed protein layer in different ways. This technique is commonly called contrast variation. Thus, when the solution is made from water consisting of approximately one mole of D_2O and two moles of H_2O, which has a scattering length density close to that of silicon, the specular reflectivity is largely caused by the adsorbed protein layer. Under these circumstances, neglecting the small contribution from the oxide layer on the surface of silicon and assuming a model of a uniformly distributed protein layer, the area per molecule A can be deduced directly from the derived scattering length density ρ and thickness of the layer τ using

$$A = \frac{\sum m_i b_i}{\rho\tau} \quad (4)$$

where m_i is the number density of component i with scattering length b_i. The values of m_i and b_i depend on the chemical composition of the protein. The surface excess Γ is related to A by

$$\Gamma = \frac{1}{N_a A} \quad (5)$$

where N_a is the Avogadro's constant. Although Fourier transformation could be used to determine the interfacial scattering length density profile, the practical procedure for extracting structural information from experimental profiles is to fit models to the data. A structural model is assumed, and the corresponding reflectivity is calculated using the optical matrix formula.[27] The calculated reflectivity is then compared with the measured one, and the structural parameters subsequently modified in a least-squares iteration to obtain a good fit. The parameters used in the calculation are the thicknesses of the layers τ_i and the corresponding scattering length densities ρ_i. Because the scattering length density of a given layer varies with isotopic composition, the fitting of a set of isotopic compositions to a single structural model greatly reduces the possibility of ambiguity in the interpretation, although it adds to the complexity of the fitting procedure. Although a single uniform layer model may not be thought to be appropriate for protein structure determination, it is usually sufficiently accurate for the determination of the adsorbed amount (*i.e.*, (Γ or A)).[28] If protein adsorption results in a uniform layer, the volume fraction of the protein in the layer ϕ_p can be obtained directly using the following equation:

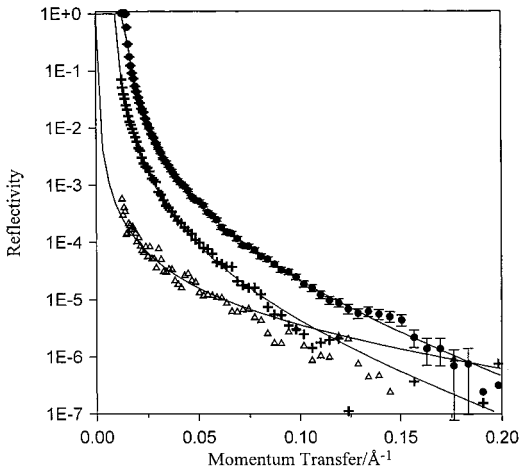

Figure 1. Neutron reflectivities as a function of momentum transfer κ at the silica-water interface using different water contrasts: (●) D_2O, (+) CM4 (scattering length density of water = 4.0×10^{-6} Å^{-2}), and (△) CMSi (scattering length density = 2.07×10^{-6} Å^{-2}). The continuous lines were calculated using the optical matrix method with an oxide layer thickness of 12 ± 3 Å.

$$\rho = \phi_p\rho_p + (1 - \phi_p)\rho_w \quad (6)$$

where ρ_w is the scattering length density of the bulk water. The surface excess of the protein in the adsorbed layer can be expressed as

$$\Gamma = \frac{\tau(1 - \phi_p)}{n_w V_w N_a} \quad (7)$$

where τ is the thickness of the protein layer, n_w is the number of water molecules associated with each protein molecule, and V_w is the water molecular volume. The value of n_w can be evaluated from the following equation

$$n_w = \frac{(1 - \phi_p)b_p}{\rho V_w - b_w(1 - \phi_p)} \quad (8)$$

where b_w and b_p are the scattering lengths for water and protein.

Results and Discussion

I. Characterisation of the Oxide Layer. Although the thickness of the thin oxide layer present on the freshly polished silicon (111) surface is always less than 30 Å thick, it is necessary to measure its thickness accurately because its signal contributes to all the reflectivities measured and it may vary in thickness and composition from block to block. The structure of the oxide layer is most reliably determined by measuring its neutron reflectivity profile with the block in contact with water using the sample cell described in the experimental section. The water helps to highlight the oxide layer, especially when it is defective. Measurements were made at three different water contrasts: D_2O, CM4 ($\rho = 4 \times 10^{-6}$ Å^{-2}) and CMSi ($\rho = 2.07 \times 10^{-6}$ Å^{-2}). The sensitivity of the reflectivity profiles to the contrast variation is demonstrated in Figure 1. The reflectivity is weakest for CMSi because the signal is only from the oxide layer. In D_2O the total scattering length density of

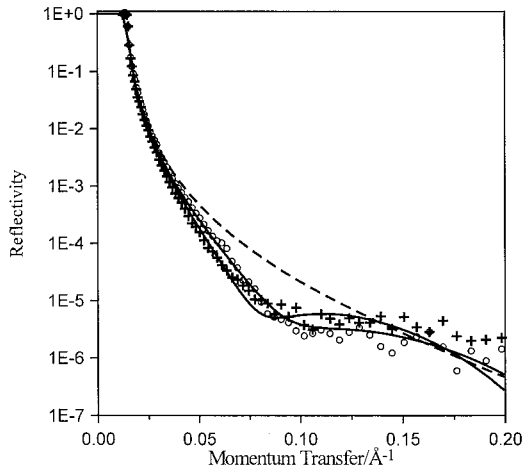

Figure 2. Plots of neutron reflectivity profiles at the silica−D_2O interface at BSA concentrations of 0.005 *g dm*$^{-3}$ (○) and 0.15 *g dm*$^{-3}$ (+). The solution pH was 5.1 and the ionic strength was 0.02 *M*. The reflectivity from the bare silicon oxide−D_2O interface is also shown for comparison (dashed line).

the oxide layer would be higher than that of pure silica (3.41×10^{-6} Å^{-2}) if any water penetrates into the layer. However, all the reflectivity profiles were fitted using a thickness of 12 ± 3 Å and $\rho = 3.41 \times 10^{-6}$ Å^{-2} for the oxide layer. No penetration of water into the layer was found and this is consistent with the scattering length density of the layer being exactly as expected for amorphous oxide. Furthermore, no roughness was necessary to fit the reflectivity, suggesting that the oxide surface is also quite smooth. The quality of the surface on this silicon block is thus better than the oxide surface used in the previous study, although this is not expected to affect protein adsorption.

II. BSA Adsorption Isotherm at pH 5.1. The isoelectric point (IEP) for BSA is at pH 4.8, and it has been reported that the surface excess attains its maximum value at this point.[1] Before examining the effects of pH on the surface adsorption, it is of interest to examine the variation of surface excess with bulk protein concentration in the region of the IEP. The amount of BSA adsorbed on the silicon oxide surface was determined by measuring neutron reflectivity profiles in D_2O because D_2O highlights any adsorbed protein at the solid surface. Figure 2 shows the variation of neutron reflectivity with BSA concentration for a set of BSA concentrations at pH 5.1. The effect of bulk BSA concentration on the adsorbed surface layers can be seen by comparing the reflectivities with that from the bare silica/D_2O interface, which is shown as a dashed line in Figure 2. BSA adsorption results in a lowering of reflectivity compared with that from the bare solid−D_2O interface. The shape of the reflectivity profiles in the presence of BSA also changes with BSA concentration, indicating increasing BSA adsorption. Because the adsorption with respect to protein concentration is known to be largely irreversible, the measurements were made in order of increasing BSA concentration.

The amount of protein adsorbed (surface excess) can be obtained by fitting a uniform layer model to the reflectivity profiles using the optical matrix formalism already outlined. The continuous lines in Figure 2 were calculated for a uniform layer of protein adsorbed on the silicon oxide layer, assuming the structure of the oxide layer to be as already determined in pure water. The volume fraction and surface excess of the adsorbed protein in the surface layer can be calculated using eqs 5−8, and the value of the scattering length density of pure protein given in Table 1. The variation of scattering length density with the ratio of H_2O and D_2O reflects the exchange of

TABLE 1: Scattering Length Densities of BSA in Different Water Contrasts[a]

pH	3	5.1	7
$D_2O \times 10^6$/Å^{-2}	3.34	3.33	3.24
CM4 $\times 10^6$/Å^{-2}	2.83	2.79	2.78
CMSi $\times 10^6$/Å^{-2}	2.41	2.41	2.41
$H_2O \times 10^6$/Å^{-2}	1.85	1.90	1.90

[a] The total molecular volume was taken to be 79111 Å^3 (see ref 38). The degree of ionization of different amino acid groups was taken from ref 39.

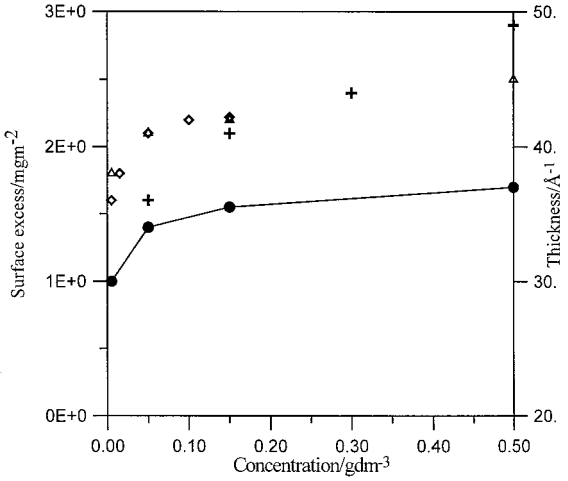

Figure 3. Surface excesses (△) and layer thicknesses (●) obtained from the uniform layer model plotted as a function of BSA bulk concentration. The solution pH was 5.1 and the ionic strength was 0.02 *M*. The surface excesses obtained by Norde *et al.*[29] (◇) and Kondo *et al.*[12] (+) are also shown for comparison.

labile hydrogens within BSA molecules with bulk water. The values listed in Table 1 were calculated assuming that the exchange was complete, an assumption which will be justified later. The good fit of the single uniform layer model to the measured reflectivity profiles indicates the correctness of the model. The poor fit over the higher κ range at 0.15 *g dm*$^{-3}$ was due to the uncertainty of background subtraction and the level of difference between the measured and calculated curves was within acceptable error. The thicknesses obtained, which are plotted in Figure 3, show a small increase at low concentration which soon reaches a plateau with a maximum layer thickness slightly shorter than the length of the minor axis of 40 Å for the BSA globular structure. At this stage we note that the thickness of the layer is about what would be expected for sideways-on adsorption. The surface excesses at pH 5.1 are also plotted as a function of BSA concentration in Figure 3. The surface excess reaches its maximum value at low concentrations, suggesting that it has a high affinity for the hydrophilic silicon oxide surface. The surface excess tends to a limit of 2.5 *mg m*$^{-2}$ at a bulk concentration of 0.5 *g dm*$^{-3}$, corresponding to an area per molecule of 4400 Å^2. If it is assumed that the BSA molecule is rigid the cross sectional area for close packed sideways-on adsorption is 5600 Å^2 (40 × 140 Å), corresponding to a limiting surface excess of only 2 *mg m*$^{-2}$. That the limiting molecular area at maximum adsorption is smaller than the minimum area required for sideways-on adsorption suggests that there may be some deformation of the globular structure, which we discuss further below.

BSA adsorption at the silica/water interface has been studied by Norde *et al.* on a particulate adsorbent.[29] The surface excess was obtained by titrating BSA solutions before and after equilibration with the silica particles. The surface excesses up

to 0.15 *g dm*$^{-3}$ are compared with our values in Figure 3. Within this lower concentration range these results are in excellent agreement with the neutron values. A similar study using silica powder has also been carried out by Kondo *et al.*[12] Their BSA surface excesses, also shown in Figure 3, have a more pronounced increase with bulk concentration, but are still in acceptable agreement with the neutron results if the combined errors are taken to be 15%. Comparison with studies of BSA adsorption on other surfaces makes it possible to examine the effect of surface properties on BSA adsorption. The surface most closely related to silica is probably the bare mica surface. Fitzpatrick *et al.*[13] measured the amount of BSA adsorbed onto mica by preadsorbing BSA onto mica and by measuring the *x*-ray photoelectron spectra (XPS) of the dried surface under vacuum. The surface excess was found to be 5.7 ± 1 *mg m*$^{-2}$ at a bulk BSA concentration of 0.005 *g dm*$^{-3}$, compared with the neutron value of 1.8 *mg m*$^{-2}$. In a parallel study at the same solution concentration using a surface force apparatus, Fitzpatrick *et al.* estimated the level of surface excess to be 5.5 to 6.5 *mg m*$^{-2}$, which is consistent with their XPS result, but is 3 times greater than the neutron finding. Fitzpatrick *et al.* also claimed that their result is comparable with early work by Clark *et al.*[6] on thin liquid films formed by BSA. Adsorption of BSA on the hydrophilic surface of an optical waveguide made of mixed titanium oxide and silicon oxide at pH 7.4 has also been studied recently by Kurrat *et al.*[30] using the integrated optical signal. When saturation was reached after about an half-hour the BSA surface excess at a bulk concentration of 0.084 *g dm*$^{-3}$ was found to be 1.5 *mg m*$^{-2}$. This value is close to the values given in Figure 3, but when allowance for the effects of pH is made, their surface excess is relatively higher. There are also several studies on BSA adsorption on polymer surfaces, which show that the pattern of BSA adsorption is strongly affected by surface charge and hydrophobicity.[4]

There is some value in comparing the BSA adsorption with that from HSA (human serum albumin) because HSA has almost the same molecular weight, IEP, globular dimensions, and other physical properties as BSA.[31] HSA also has 86% of its amino acid sequence identical to BSA. A recent study of HSA adsorption on mica by Blomberg *et al.*[32−33] using XPS over the HSA concentration range from 10^{-3} to 1 *g dm*$^{-3}$ at pH 5.5 found that adsorption reaches a saturation limit of 2.5 *mg m*$^{-2}$ at 0.005 *g dm*$^{-3}$. The surface excess then remains constant until an HSA concentration of about 0.01 *g dm*$^{-3}$, after which there is a further increase. Koutsoukos *et al.*[34] studied the adsorption of human plasma albumin (HPA) on different solid particles at pH 4.7 and found a maximum surface excess for the adsorption on the positively charged haematite (α-Fe_2O_3) at 2.7 *mg m*$^{-2}$ for protein concentrations above 0.3 *g dm*$^{-3}$, close to our value for the saturation limit for BSA on the negatively charged silicon oxide surface. However, their values for the adsorption of the same protein on charged polystyrene particles suggest that adsorption reaches saturation at higher bulk protein concentrations and for a lower maximum surface excess than in the haematite system. Thus, the maximum surface excess on a positively charged polystyrene surface is 2 *mg m*$^{-2}$ as compared with 2.3 *mg m*$^{-2}$ on a negatively charged polystyrene surface. Finally, we note that, although HSA and BSA are similar in many of their physical properties, their surface activities appear to be different. Kurrat *et al.*[30] recently compared the adsorption of BSA and HSA onto the hydrophilic Si (Ti)O_2 surface from aqueous solution and found that at a protein concentration of 0.084 *g dm*$^{-3}$ and pH 7.4 the saturated surface excess for HSA was 2.4 *mg m*$^{-2}$ as compared with 1.3 *mg m*$^{-2}$ for BSA, a difference of almost a factor of 2. The difference in surface adsorption must stem from the difference in secondary and tertiary structures caused by the 14% deviation in amino acid sequence.

The driving force for these protein molecules to adsorb onto the solid-water interfaces has been discussed by Norde[4] and Blomberg et al.[32−33] At a pH close to the IEP the surface is negative but the protein molecules are approximately neutral. Surface induced conformational changes upon adsorption may lead to a gain of entropy for the system. Also, even when the overall charge on BSA is zero the charge and hydrophobicity within each domain of the protein may be different[20] and the negatively charged surface may attract the polar and positively charged portions of the BSA, inducing structural deformation.

III. The Effect of Solution pH. Because BSA contains a large number of groups which can ionise under different pH conditions, a change in pH is expected to affect the surface affinity of BSA. In studying HSA adsorption on charged polystyrene particle surfaces Norde *et al.*[1,4] found that at a given bulk concentration the HSA surface excess peaks at about its IEP, although the exact position of the maximum is affected by the charge on the particle surface. Norde *et al.*[1,4] also found indications that the surface excess is sensitive to the charge distribution on the protein. The surface excess may also decrease as a result of increasing electrostatic repulsion between protein molecules within the adsorbed layer. Furthermore, because BSA is composed of different domains, changes in pH may affect the inter- and intramolecular interactions, resulting in a variation in the shape of the protein. Using SANS Chen *et al.*[19] have demonstrated that the scattering intensity of BSA measured at pH 5.1 can be fitted using a prolate ellipsoid with a long axis of 70 ± 2 Å and a short axis of 20 ± 1 Å. However, at pH 7 the measured scattering intensity could not be fitted without taking account of the strong electrostatic interactions between BSA molecules. A change in shape of HSA with solution pH has also been demonstrated by Olivieri *et al.*[17] in a recent SAXS experiment. Thus, changes in solution pH are expected to affect the surface excess and the structural conformation of the adsorbed layer.

The effect of pH on the amount of BSA adsorbed at the silicon oxide−water interface was examined by varying the pH in D_2O. The BSA concentration was fixed at 0.15 *g dm*$^{-3}$ and the ionic strength was held at 0.02 *M*. The sequence of measurements was pH 5.1, pH 7.0, pH 5.1 (to check the reproducibility), pH 3, and back to pH 5.1. The neutron reflectivity profiles are shown in Figure 4a where the profile at pH 5.1 has the lowest reflectivity, indicating that this corresponds to the highest surface adsorption within the pH cycle. That the reflectivity profiles at the other two pHs are almost identical shows that the amount and thickness of the adsorbed BSA layers are similar for these two cases. For clarity, the reflectivity profiles measured at pH 5.1 at the three different stages of the cycle are compared separately in Figure 4b where it can be seen that they are identical within error, showing that adsorption is completely reversible with respect to pH under these conditions. The exact surface excess can be calculated using a similar model to that used before and the results are shown in Figure 5 where the maximum surface adsorption at pH 5.1 can be clearly seen. The surface excess at pH 3 and 7 was found to be about 0.5 *mg m*$^{-2}$ as compared with 2.5 *mg m*$^{-2}$ at pH 5.1. The thickness at pH 3 and 7 is 30 ± 3 Å, compared with 36 ± 3 Å at pH 5.1. Given that the surface excess at pH 3 and 7 is very lower the oxide surface is unlikely to be fully covered by BSA molecules. However, the measure-

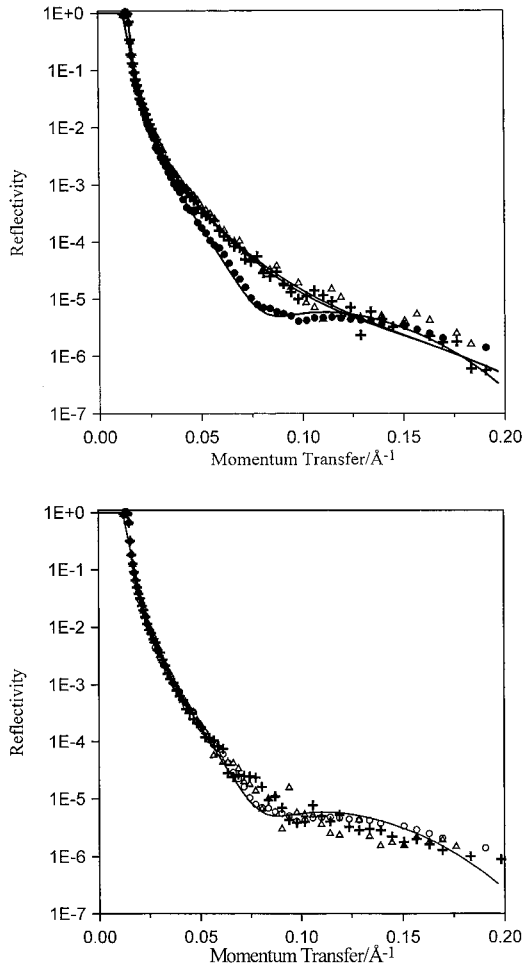

Figure 4. Effect of pH on BSA adsorption measured as the variation of reflectivity in D_2O at 0.15 *g dm*$^{-3}$. The adsorption was started at pH 5.1, then raised to 7, followed by 5.1, then lowered to 3, before returning to 5.1. (a) The comparison of the reflectivity profiles measured at pH 5.1 (●), (+), and 3 (△). (b) The three reflectivity profiles at pH 5.1 (the pH sequence is (○), (+), and (△)). The continuous line is the average fit to the three profiles with a BSA layer thickness of 30 Å.

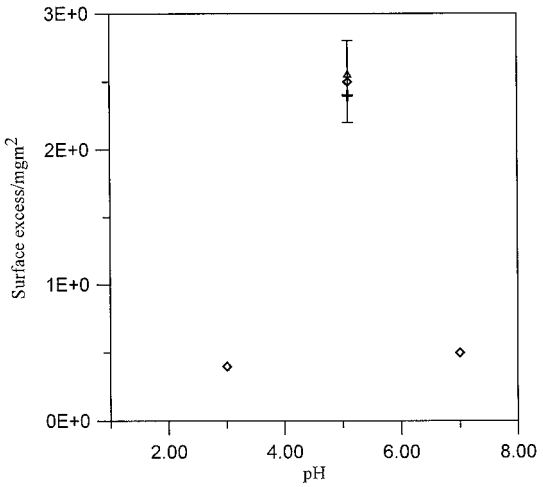

Figure 5. Effect of pH on the surface excess of adsorbed BSA in D_2O at 0.15 *g dm*$^{-3}$. The solution pH was initially 5.1 (◇) then raised to 7 (◇), followed by 5.1 (+), then lowered to 3 (◇), before returning to 5.1 (△). The results suggest completely reversible adsorption.

ment of specular reflection is only sensitive to the depth distribution and is insensitive to the in-plane distribution at all.

Although it is well known that adsorption of many proteins with respect to bulk concentration is largely irreversible, the nature of adsorption with respect to pH has not been as well studied. There are two factors that tend to lead to irreversible adsorption with respect to concentration. First, adsorption leads to a number of direct contacts with the solid surface which may, for example, result in the formation of hydrogen bonds between the hydroxy groups on the solid surface and those on the outer surface of the protein. Although the bonding energy of such an individual bond may be relatively weak, reversible adsorption will require the simultaneous breaking of all contacts and this is energetically high with respect to the driving force for desorption. Second, adsorption may cause some structural deformation which results in a positive contribution to the entropy of adsorption. This would mean that additional energy is required to cause desorption. Such structural changes in the adsorbed BSA have been found by Kondo *et al.* using transmission circular dichroism[12] who showed that adsorption onto silica particles resulted in a substantial loss of α-helix content compared with the native structure. Subsequent desorption of the BSA by displacement with morpholine led to the recovery of almost all of the α-helix structure, suggesting that the desorbed molecules recover their native globular structure. These results were supported by the work of Norde *et al.*[29] using the same technique, although Norde *et al.* showed that some fraction of the α-helix content from the desorbed BSA was lost. It is possible that morpholine may interact with BSA in a similar manner to surfactants, causing some loss in tertiary structure.

The present neutron results suggest that adsorption and desorption with respect to pH is reversible and no permanent damage is caused to the globular structure. The actual surface excesses observed at different pH are determined by the balance of the interaction between protein molecules and the solid surface and the lateral interaction between the adsorbed protein molecules. The complete reversibility with respect to pH suggests that electrostatic interactions may be sufficient to overcome any energy barrier created by the attachment of the different fragments onto the solid surface or any entropy gain caused by structural deformation following adsorption. However, the similar values of the surface excess at pH values above and below the IEP indicate, however, that the situation is more complex. The oxide surface is negatively charged above pH 2 and according to Iler[35] the negative charge density is almost constant over pH 3−8. Thus, below the isoelectric point of 4.8 the driving force for surface adsorption is likely to be the electrostatic attraction of the positively charged BSA. As the pH is decreased the net positive charge on BSA increases and with it the lateral repulsion, leading to a reduction in the amount adsorbed. However, above the IEP, both the BSA and the solid surface are negatively charged and adsorption must be driven by the entropy gain caused by dehydration and/or the conformational entropy gain resulting from the loss of secondary and tertiary structure. The decrease of surface excess with increasing pH again could indicate that electrostatic repulsion within the adsorbed BSA layer limits the surface coverage, but the similar values of the surface excess on either side of the IEP at pH 3 and 7 suggest that the contribution of electrostatic attraction between surface and protein layer both above and below the IEP may not be the main factor causing adsorption.

IV. Structure of BSA Layers. The globular BSA molecule contains three main domains which can be further divided into six subdomains and in comparison with single domain globular proteins the stability of its tertiary structure is weak. Upon adsorption, direct contacts will be established between BSA and the solid surface and the formation of such contacts may cause

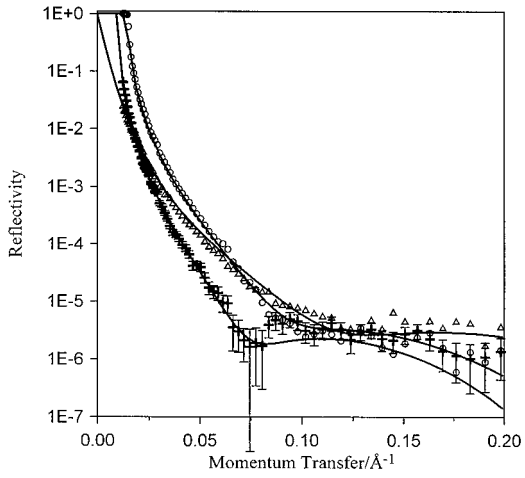

Figure 6. Single uniform layer fits to the reflectivity profiles at pH 5.1 in the presence of 0.005 *g dm*$^{-3}$ BSA: (○) D_2O, (+) CM4, (△) H_2O. The continuous lines were calculated using $\Gamma = 1.85$ *mg m*$^{-2}$ and $\tau = 30$ Å.

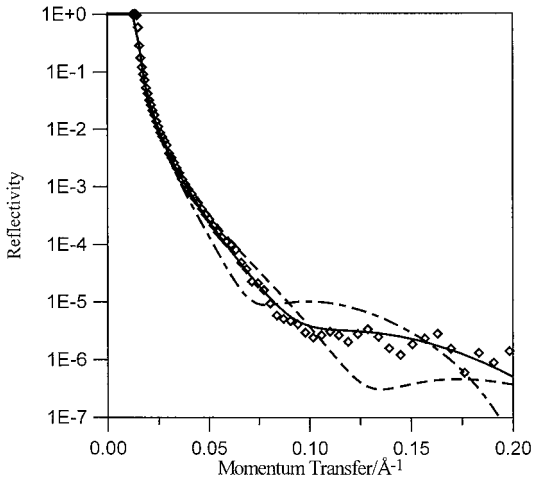

Figure 7. Single uniform layer fits to the reflectivity profile in D_2O at pH 5.1 in the presence of 0.005 *g dm*$^{-3}$ BSA. The continuous lines were calculated using $\tau = 20$ Å (dashed line), 30 Å (continuous line), and 40 Å (dashed and dotted line).

deformation of the protein molecules with the consequent loss of α-helix or *β*-sheet structure, which may then generate further contacts. Since BSA contains 17 disulphide bridges the native structure within each subdomain will be kept in a reasonably ordered state in aqueous solution, but this is unlikely to be the case for the three main domains. The measured thickness of the adsorbed protein layer can be combined with the known globular dimensions of BSA under different solution conditions to assess the orientation of the protein molecules on the surface and the extent of structural deformation caused by the contact with the solid wall. Blomberg *et al.*[32−33] have used this approach to examine the structural conformation of HSA at the solid-water interface using surface force measurements. The advantage of neutron reflection over other techniques is that it is more sensitive to the structural distribution normal to the interface and can probe interfacial layer thickness with a resolution of a few angstroms. This is especially the case if the measurements can be made under different water contrasts. Although measurements in D_2O provide good quality information about the adsorbed amount of BSA, they are less effective in revealing unambiguous structural distributions.[28] However, the use of a range of water contrasts serves to highlight different regions of the interface and hence greatly reduces any ambiguities associated with the fitting of single reflectivity profiles.

Figure 6 shows the reflectivity from a 0.005 *g dm*$^{-3}$ BSA solution at pH 5.1 at three different water contrasts. We have attempted to fit all the reflectivity profiles using the same single uniform layer model for the protein layer as that used for extracting surface excess shown in Figure 2 and the continuous lines in Figure 6 are the best fits using a thickness of 30 ± 3Å for the protein layer. The scattering length densities were calculated using the fixed protein volume fraction of 0.44 obtained earlier and the residual space was filled with water of the appropriate contrast. The single oxide layer was taken to be the same as that of the bare surface shown in Figure 1 and no roughness was included in the fitting. In the calculation of the scattering length of the protein complete exchange of the labile hydrogens in BSA with the bulk water was assumed. This is an important assumption which we now consider in more detail.

The extent of exchange of the labile hydrogens in BSA with D_2O has been extensively investigated in the past and has been reviewed by Hvidt and Nielsen.[36] Most of these exchange experiments are aimed at revealing the mechanisms relating to the folding and unfolding of protein molecules under different solution conditions. Typically, the accessibility of hydrogen atoms to exchange with those from the surrounding water has been used as a measure of the masking of portions of the polypeptide. Of some 1015 potentially labile hydrogen atoms per BSA molecule, about 750 exchange almost instantly at pH 7 and 0 °C. A further 250 exchange over a period of a few minutes up to 2 h. The remaining 30−50 appear not to exhange within a further 24 h. Thus, over 90% of the labile hydrogens are readily exchangable. Hvidt and Nielson also found that the exchange was pH dependent with all of the labile hydrogens exchanging below pH 3.5 and above pH 9. Increase in temperature also substantially accelerates the exchange rate. The most difficult hydrogens to exchange are those on the amide groups on the peptide chain, of which BSA has 582. The barrier preventing the exchange is the hydrophobic encapsulation of any labile hydrogens inside the globular structure but, because most of the labile hydrogens in the peptide chain are on the outer surface of the globular structure, they are easily exchanged. Only a small fraction are expected to be buried. Structural deformation accompanying adsorption may cause sufficient disturbance to the encapsulated peptide chain fragments to allow exchange to proceed to completion. Uncertainty in the extent of exchange introduces an error into the scattering length of BSA and this error will vary with the different water contrasts. A 5% error in scattering length will generally carry over to be an equivalent error in the derived surface excess. Since the difference in scattering length for the labile hydrogens is largest in D_2O the effect caused by incomplete exchange will be largest for the D_2O measurements but much less for the other contrasts. That all the reflectivity profiles measured under different water contrasts at a given concentration can be fitted accurately by the same structural profile indicates that, in the present case, the level of uncertainty caused by hydrogen exchange falls within the other errors of the experiment. It is also important to realize that any uncertainty in scattering length has no effect at all on the derived layer thickness.

An assessment of the reliability of the fitted layer thickness can be made by comparing the measured reflectivity with profiles calculated for different thicknesses. Figure 7 compares the measured reflectivity in D_2O at 0.005 *g dm*$^{-3}$ with profiles calculated for thicknesses of 20, 30, and 40 Å, in each case the scattering length density having been adjusted to give the best fit. The reflectivity profile at the thickness of 30 Å is a

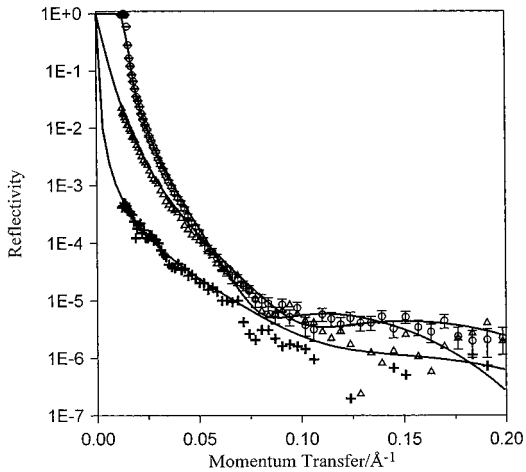

Figure 8. Single uniform layer fit to the measured reflectivity at pH 5.1 in the presence of 0.15 *g dm*$^{-3}$: (○) D_2O, (+) CMSi, and (△) H_2O. The continuous lines were calculated using $\Gamma = 2.5$ *mg m*$^{-2}$ and $\tau =$ 36 Å. The result suggests sideways-on monolayer adsorption.

significantly better fit than the others and demonstrates the sensitivity of the technique to the thickness of the adsorbed layer. Indeed, as the surface excess increases the measured reflectivity becomes more sensitive towards layer thickness.

The structure of the layer may change with the surface concentration and this was found to be the case for lysozyme adsorption at the hydrophilic silicon oxide−water interface.[2] For example, at pH 7, the lysozyme adsorbed sideways-on at 0.03 *g dm*$^{-3}$ but bilayer adsorption occurred when the concentration was increased to 1 *g dm*$^{-3}$. Possible structural changes of the BSA layer with concentration were assessed using a set of measurements in different water contrasts at 0.15 *g dm*$^{-3}$. Figure 8 shows the measured reflectivity profiles in D_2O, CMSi, and H_2O for this concentration together with the best fits to the data. It was once again found that the reflectivity profiles for different water contrasts were well fitted using the single uniform layer model for the adsorbed BSA layer but with an increased layer thickness of 36 Å, an increase of 20%, and a smaller percentage increase in the BSA volume fraction.

The pattern of formation of the monolayer over the concentration range studied gives no indication of denaturation in that there is no fragmentation in the distribution of the layer along the surface normal. Fragmentation of the layer would be expected to give a gradient in the volume fraction of protein with the highest volume fraction next to the surface, as we have observed at hydrophobic surfaces.[15] This would necessitate the division of the adsorbed layer into two or more layers of unequal scattering length density, which would be readily seen in the fitting of the data. That there is no denaturation is also consistent with adsorption being reversible with respect to pH variation.

The thickness of the adsorbed BSA layer is close to the length of the short axis of the BSA molecules and this then suggests that the monolayer consists of molecules adsorbed sideways-on to the surface. Because the structure of the BSA molecule is commonly given as a string of three spherical domains, the similarity in thickness of the layer with the dimension of the short axis of 40 Å shows that the molecule must be lying flat on the surface. The question then arises as to whether it is appropriate to compare the observed thickness of a *uniform* layer directly with the diameter of the BSA *cylinder*. The uniform layer would be expected to give a value slightly smaller than the theoretical value of 40 Å because of the averaging effect. However, in separate experiments on the more robust globular lysozyme,[2] where no change in geometry is expected on adsorption, the uniform layer thickness was found to be the same as the appropriate globular dimension, indicating that the averaging effect is small and may be compensated by a small roughness of the underlying surface. The decrease from 40 to 30 Å is therefore large enough to show that there is some structural deformation of the BSA on adsorption and some may still remain at the higher surface concentration where the uniform layer thickness is 36 Å. Carter *et al.*[31] have shown that slight conformational changes in serum albumin may result in reduction of the short axial length of the globular structure and structural deformation on the oxide surface has also been discussed by Norde *et al.*[29]

As already demonstrated by the various calculated profiles in Figure 7, the measured reflectivities cannot in any way be explained in terms of a head-on adsorbed monolayer. This contradicts the finding of the surface force measurement by Fitzpatrick *et al.*[13] who suggested that BSA adsorption on mica was in the form of a complete head-on monolayer with a layer thickness of 120 Å. It is possible that mica has quite different adsorptive properties from silica but it would be surprising if the differences were as large as apparently observed. No information was given in the work by Fitzpatrick *et al.* concerning the origin and purity of their BSA sample, although impurities such as fatty acids can cause serious distortion of the shape of the BSA assembly and strongly affect its surface activity.[20] A similar surface force study was made by Gallinet *et al.*[14] under almost identical conditions. Gallinet *et al.*[14] found three steps each of about 44 Å in the surface force−distance curve, suggesting that the adsorbed layer was composed of three sideways-on BSA molecules. The surface force was monitored by bringing the two adsorbed mica surfaces towards each other and such a measurement is very sensitive to the maximum dimension of an adsorbed layer. Given this sensitivity of the surface force apparatus, it is not unreasonable to expect the force variation with distance to reflect the displacement of any loosely attached outer layers. The neutron reflection results do not necessarily contradict this observation because the outer layers would only be detected if their volume fractions were sufficiently high. The combined results would then suggest that the volume fractions in the outer layers must be very low.

The adsorption of HSA on a mica surface has been studied by Blomberg *et al.*[32−33] using the surface force apparatus. These authors showed that the adsorbed HSA layers are more compressible than single domain proteins like insulin and lysozyme, suggesting a lack of conformational stability in the HSA layer. The layer thickness below 0.01 *g dm*$^{-3}$ was found to be between 30 and 35 Å, suggesting sideways-on adsorption, an observation in good agreement with our neutron findings. Blomberg *et al.* also observed that as the HSA concentration was increased to 1 *g dm*$^{-3}$ the adsorbed layer thickness increased from 30 to 120 Å, indicating that the adsorbed layer switched from a sideways-on conformation to predominantly head-on adsorption. Further neutron measurements are now in progress to extend the current work to cover the higher BSA concentration range.

Conclusions

The high interfacial resolution of specular neutron reflection has enabled us to determine the *in situ* protein layer distribution at the solid-water interface. The use of isotopic substitution to vary the water contrast limits the number of possible models that will fit the set of reflectivity data thus adding confidence in the correctness of the chosen model. The uniformity of the

adsorbed BSA layer at each concentration is supported by the combined measurements under several different water contrasts. This information together with the molecular geometry of native BSA suggests that the adsorbed layer adopts a sideways-on conformation over the whole concentration range studied. That the thicknesses of the adsorbed layers are all less than the length of the short axis of the protein indicates that there is some structural deformation or flattening of the molecule caused by the interaction with the solid surface. The observed structural deformation is consistent with the findings from surface force measurements which indicate a high surface compressibility of the BSA. The extent of BSA deformation contrasts with the unchanged thickness of lysozyme when adsorbed sideways-on at the same interface.

The sensitivity of neutron reflectivity allows us to monitor the variation of surface excess with respect to pH. The results suggest that adsorption with respect to pH cycling is completely reversible. The reversibility of the adsorption is a good indication that structural deformation does not lead to irreversible damage to the adsorbed BSA.

Although many studies have been made of albumin adsorption and its subsequent interaction with other biological molecules the current study represents the most thorough characterisation of the physical properties of an adsorbed BSA layer. That BSA adsorption forms a smooth and densely packed monolayer over a wide bulk concentration range may be of practical significance. It has been known for a long time that albumin is a harmless and inert protein, and its adsorption on foreign surfaces can prevent activation of proteolytic enzymes, *e.g.*, blood coagulation factors or complement proteins. A preadsorbed albumin layer could also block the direct exposure of other more harmful proteins including IgG and fibrinogen to the surfaces of medical devices or implants.

Acknowledgment. We thank the Biotechnology and Biological Sciences Research Council for support.

References and Notes

(1) Haynes, C. A.; Norde, W. *Colloids Surf., B* **1994**, *2*, 517.
(2) Su, T. J.; Lu, J. R.; Thomas, R. K.; Cui, Z. F.; Penfold, J. *Langmuir*, **1998**, *14*, 438.
(3) Horbett, T. A.; Brash, T. A. *Protein at Interfaces II*; ACS Symposium Series 602; Washington, DC, 1995.
(4) Haynes, C. A.; Sliwinski, E.; Norde, W. *J. Colloid Interface Sci.* **1994**, *164*, 394.
(5) Rapola, R. J.; Horbett, T. A. *J. Colloid Interface Sci*. **1990**, *136*, 480.
(6) Clark, D. C.; Coke, H.; Mackie, A. R.; Pinder, A. C.; Wilson, D. C. *J. Colloid Interface Sci.* **1990**, *138*, 207.
(7) Baszkin, A.; Boissonnade, M. M. *J. Biomed. Mater. Sci.* **1993**, *27*, 145.
(8) Malmsten, C. *J. Colloid Interface Sci*. **1994**, *166*, 333.
(9) McGuire, J.; Wahlgren, M.; Arnebrant, T. *J. Colloid Interface Sci.* **1995**, *170*, 182.
(10) Liebmann-Vinson, A.; Lander, L. M.; Foster, M. D.; Brittain, W. J.; Vogler, E. A.; Majkrzak, C. F.; Satija, S. *Langmuir*, **1996**, *12*, 2256.
(11) Haynes, C. A.; Norde, W. *J. Colloid Interface Sci.* **1995**, *169*, 313.
(12) Kondo, A.; Oku, S.; Higashitani, K. *J. Colloid Interface Sci.* **1991**, *143*, 214.
(13) Fitzpatrick, H.; Luckham, P. F.; Eriksen, S.; Hammond, K. *Coll. Surf.* **1992**, *65*, 43.
(14) Gallinet, J.; Gauthier-Manuel, B. *Coll. Surf.* **1992**, *68*, 189.
(15) Lu, J. R.; Su, T. J.; Thirtle, P.; Thomas, R. K.; Rennie, A. R. *J. Colloid Interface Sci.* **1998**, *203*, 419.
(16) Anderegg, J. W.; Beeman, W. W.; Shulman, S.; Kaesberg, P. *J. Am. Chem. Soc.* **1955**, *77*, 2927.
(17) Olivieri, J. R.; Craievich, A. F. *Eur. Biophys. J*. **1995**, *24*, 77.
(18) Doherty, P.; Benedek, G. B. *J. Chem. Phys.* **1974**, *61*, 5426.
(19) Bendedouch, D.; Chen, S. H. *J. Phys. Chem.* **1983**, *87*, 1473.
(20) Peters, T. *Adv. Protein Chem.* **1985**, *37*, 161.
(21) Penfold, J.; Richardson, R. M.; Zarbakhsh, A.; Webster, J. R .P.; Bucknall, D. G.; Rennie, A. R.; Jones, R. A. L.; Cosgrove, T.; Thomas, R. K.; Higgins, J. S.; Fletcher, P. D. I.; Dickinson, E.; Roser, S. J.; McLure, I. A.; Hillman, R. A.; Richards, R. W.; Staples, E. J.; Burgess, A. N.; Simister, E. A.; White, J. W. *J. Chem. Soc., Farada6 Trans.* **1997**, *93* 3899.
(22) Fragneto, G.; Lu, J. R.; McDermott, D. C.; Thomas, R. K.; Rennie, A. R.; Gallagher, P. D.; Satija, S. K. *Langmuir* **1996**, *12*, 477.
(23) Brzoska, J. B.; Shahidzadeh, N.; Rondelez, F. *Nature* **1992**, *360*, 719.
(24) Vig, J. R. *J. Vac. Sci. Technol.* **1985**, *A3*, 1027.
(25) Lu, J. R.; Lee, E. M.; Thomas, R. K. *Acta Cryst.* **1996**, *A52*, 42.
(26) Crowley, T. L. *Physica A* **1993**, *195*, 354.
(27) Born, M., Wolf, E. *Principles of Optics*; Pergamon: Oxford, 1970.
(28) Lu, J. R.; Su, T. J.; Thomas, R. K.; Penfold, J.; Richards, R. W. *Polymer*, **1996**, 37, 109.
(29) Norde, W.; Favier, J. P. *Coll. Surf.* **1992**, *64*, 87.
(30) Kurrat, R.; Prenosil, J. E.; Ramsden, J. J. *J. Colloid Interface Sci.* **1997**, *185*, 1.
(31) Carter, D. C.; Ho, J. X. *Adv. Protein Chem.* **1995**, *45*, 153.
(32) Blomberg, E.; Claesson, P. M.; Tilton, R. D. *J. Colloid Interface Sci*. **1994**, *166*, 427.
(33) Blomberg, E.; Claesson, P. M.; Golander, C. G. *J. Dispersion Sci. Tech.* **1991**, *12*, 179.
(34) Koutsoukos, P. G.; Mumme-Young, C. A.; Norde, W.; Lyklema, J. *Coll. Surf.* **1982**, *5*, 93.
(35) Iler, R.K. *The Chemistry of Silica* Wiley: New York, 1979.
(36) Hvidt, A.; Nielsen, S. O. *Adv. Protein Chem.* **1966**, *21*, 287.
(37) Claesson, P. M.; Blomberg, E.; Froberg, J. C.; Nylander, T.; Arnebrant, T. *Adv. Colloid Interface Sci.* **1995**, *57*, 161.
(38) Van Krevelen, D. W. *Properties of Polymers* 3rd ed.; Elsevier: New York 1990.
(39) Stryer, L. *Biochemistry*, 3rd ed.; W. H. Freeman and Company: New York, 1988.